Cell Tissue Res (2003) 311:31–45
DOI 10.1007/s00441-002-0653-5

REGULAR ARTICLE

**Sabine Fuchs · Andrew John Hollins · Michael Laue
Ulrich Friedrich Schaefer · Klaus Roemer
Mark Gumbleton · Claus-Michael Lehr**

Differentiation of human alveolar epithelial cells in primary culture: morphological characterization and synthesis of caveolin-1 and surfactant protein-C

Received: 25 March 2002 / Accepted: 8 October 2002 / Published online: 12 November 2002

Abstract Human alveolar type II cells were isolated from lung tissue and cultured for several days. The morphology of cells was investigated at different time points postseeding and the synthesis of alveolar cell-type specific proteins was analyzed using different methods. The rationale of the study was to characterize a primary cell culture of human alveolar cells for the development of an in vitro model studying pulmonary drug delivery. In vitro test systems based on human cells are attracting increasing interest as important alternatives to animal-derived models because possible interspecies differences in alveolar cell biology and transport mechanisms cannot be excluded. In our study, both morphological characterization and marker protein synthesis of human alveolar cells in culture indicate the differentiation of isolated alveolar type II cells into epithelial monolayers consisting of alveolar type I-like and alveolar type II-like cells, which corresponds to the composition of the alveolar epithelium of the donor tissue. By using flow cytometry, immunofluorescence, immunoblotting and reverse transcriptase polymerase chain reaction (RT-PCR), we observed a shift in the synthesis of important marker proteins. Early cultures were characterized by low caveolin-1 and high Sp-C levels. In comparison, the protein biosynthesis of alveolar cells switched with time of culture to high caveolin-1 and low Sp-C levels. Based on the similarity between human alveolar epithelium and the development of our primary alveolar cell culture, we suggest that the culture may serve as a suitable model to study epithelial transport or cell biological processes in human alveolar cells.

Keywords Human alveolar epithelial cells · Caveolin-1 · Caveolae · Surfactant protein C · Flow cytometry · Immunogold electron microscopy · Cell culture

The Fonds der Chemischen Industrie and ZEBET (BgVV, Berlin) are thanked for their financial support.

S. Fuchs · U.F. Schaefer · C.-M. Lehr (✉)
Department of Biopharmaceutics and Pharmaceutical Technology, Saarland University, Saarbrücken, Germany
e-mail: lehr@rz.uni-sb.de
Tel.: +49-681-3023039, Fax: +49-681-3024677

A.J. Hollins · M. Gumbleton
Pharmaceutical Cell Biology, Welsh School of Pharmacy, Cardiff University, Wales, UK

M. Laue
Centre for Electron Microscopy, Department of Anatomy and Cell Biology, Medical Faculty, Saarland University, Homburg, Germany

K. Roemer
Department of Virology, Medical Faculty, Saarland University, Homburg, Germany

C.-M. Lehr
Department of Biopharmaceutics and Pharmaceutical Technology, Saarland University, Im Stadtwald, Geb. 8.1, PO Box 15 11 50, 66041 Saarbrücken, Germany

Introduction

Lung alveolar epithelium in vivo is composed of two specialized epithelial cell types, the squamous alveolar epithelial type I (ATI) cell, which constitutes approximately 93% of the alveolar epithelial surface area, and the surfactant-producing cuboidal alveolar epithelial type II (ATII) cell (Crapo et al. 1982). Current evidence supports the hypothesis that ATII cells serve as the sole progenitor for the ATI cells in vivo (reviewed in Uhal 1997; Fehrenbach 2001). Accordingly, isolated ATII cells in culture lose their characteristic phenotype and acquire over a 5- to 10-day period morphological and biochemical markers characteristic of ATI cells. Morphological changes during differentiation include the generation of monolayers with high transepithelial electrical resistance (>1,000 Ω cm^2) and a loss of microvilli, an increase in the cell surface area and the development of thin cytoplasmic attenuations extending away from a protruding nucleus (Cheek et al. 1989). Biochemical

changes include an increased reactivity to ATI-specific membrane components such as the apical plasma membrane component RTI(40) and VIII B2 (Dobbs et al. 1988; Danto et al. 1992; Vanderbilt and Dobbs 1998).

The isolation of ATII cells predominantly from rat and rabbit lung tissue, and their culture over time leading to a primary culture of ATI-like cells, is now an established technique for different purposes. For instance, primary ATI-like monolayer cultures have gained acceptance as an in vitro experimental model for the examination of the rate and mechanism of alveolar solute or drug transport (for review, see Mathias et al. 1996) and have also been widely exploited to study the mechanisms of alveolar epithelial cell differentiation (Danto et al. 1995; Dobbs et al. 1997; Campbell et al. 1999). However, the parallels between in vitro and in vivo ATII cell differentiation into ATI cells remain to be fully defined, and hence the term ATI-like cell is used to represent the in vitro derived phenotype.

Although the isolation of primary human alveolar cells has been described before (Cunningham et al. 1997; Alcorn et al. 1997; Rosseau et al. 2000), human primary cells are not commonly used or appropriately characterized as an in vitro model for the "blood-air barrier." Research using human alveolar cells is mostly done on cell lines, such as the continuous human lung adenocarcinoma cell line A549 (Giard et al. 1973). The A549 cell line possesses ATII cell phenotype and has been widely used as a system to study the regulation of pulmonary surfactant synthesis. However, cultured A549 cells do not undergo transition to form a phenotype similar to that of an ATI cell. Furthermore, although the A549 cell has received some attention as a monolayer culture for the study of solute transport, its cell architecture and barrier properties are quite distinct from that of an ATI cell monolayer (Godfrey 1997). Thus, an in vitro cell model of the human alveolar epithelium possessing the relevant qualities of the alveolar epithelium in situ is definitely needed. This requirement is underscored by data which indicate cell biological differences between the alveolar epithelium of humans and animals, e.g., the interspecies differences in the spatial expression of aquaporins (Kreda et al. 2001).

We have previously described the isolation of human alveolar type II epithelial cells (HAEpC) and their primary culture, which results in confluent monolayers capable of generating tight junctional complexes and high transepithelial electrical resistance (TEER). In addition, these monolayers revealed a preferential binding of lectins, which possess a high affinity for ATI cells (Elbert et al. 1999). In the present study we have extended our characterization of the primary cultures of human alveolar epithelial cells in order to follow the morphological cell change from an ATII phenotype to an ATI-like cell phenotype over time of culture. Moreover, we have examined the formation of characteristic plasma membrane structures termed caveolae and the synthesis of their major structural protein, caveolin-1, in these cells. The caveolae membrane system is of interest because of its potentially important role in macromolecule transport across the "blood-air barrier" of the lung (reviewed in Gumbleton et al. 2000), including both the clearance of endogenous protein from the airspace and the absorption of inhaled therapeutic proteins. Furthermore, caveolin-1 may carry out a role in the regulation of alveolar epithelial cell proliferation and differentiation (Campbell et al. 1999). The synthesis of caveolin-1 and the formation of caveolae are currently under discussion as a characteristic feature of an ATI-like cell phenotype in the alveolar epithelium in vivo and in vitro (Kasper et al. 1998; Newman et al. 1999; Campbell et al. 1999). In comparison surfactant proteins are restricted to the ATII phenotype; especially surfactant protein C (SP-C) is known to be synthesized with a high specificity by ATII (Phelps and Floros 1991; Kalina et al. 1992; Beers et al. 1994).

In this study morphological characterization by electron microscopy showed the transition of a cell population mainly consisting of ATII cells towards an epithelial monolayer composed of ATI and ATII cells during 8–10 days postseeding. The ATI-like cells revealed a typical flattened cell shape and characteristic invaginations of the plasma membrane resembling caveolae, which could be supported by immunogold electron microscopy using antibodies against caveolin-1, the main structural protein of caveolae. In parallel to the morphological findings, suggesting a differentiation process, an increased production of the structural protein caveolin-1 with time of culture was observed by reverse transcriptase polymerase chain reaction (RT-PCR), Western-blot and flow cytometry, whereas synthesis of alveolar type II marker Sp-C was restricted to the earlier stages of the culture.

Materials and methods

Cell culture

Primary type II alveolar cells (ATII) were isolated from human non-tumor lung tissue, which was obtained from patients undergoing lung resection. The use of human material for isolation of primary cells was reviewed and approved by the respective local Ethics Committees (State Medical Board of Registration, Saarland; Cardiff University Medical Ethics Committee). Isolation was performed according to a protocol previously described by Elbert et al. (1999), but with a slight modification of the enzymatic digestion. Briefly, the chopped tissue was digested using a combination of 150 mg trypsin type I (T-8003, Sigma, Deisenhofen, Germany) and 0.641 mg elastase (LS022795, CellSystems, St. Katharinen, Germany) in 30 ml balanced salt solution B (BSSB) for 40 min at 37°C. The ATII cell population was purified by a combination of differential cell attachment, Percoll density gradient centrifugation and magnetic cell sorting (magnetic beads M-450, Dynal, Hamburg, Germany) as previously described (Elbert et al. 1999). The isolated ATII cells were seeded at a cell density of 300,000 cells/cm^2 on collagen/fibronectin-coated polyester filter inserts (Transwell Clear, 6.5 mm diameter, 3470, Corning Costar, Bodenheim, Germany) using small airway growth medium (SAGM) (CC-3118, Cell Systems, St. Katharinen, Germany) containing penicillin (100 units/ml) and streptomycin (100 µg/ml) and with the addition of low serum (1% fetal calf serum, FCS) in order to suppress fibroblasts. Formation of function-

al tight junctional complexes and generation of confluent monolayers was routinely determined by measuring TEER using an electronic voltmeter (EVOM, WPI, Berlin, Germany). After reaching confluence the alveolar monolayers of HAEpC typically revealed TEER values of 1,000–2,000 Ω cm^2 on day 6–8 post-seeding. The formation of tight junctions was also routinely monitored by immunolabeling for zonula occludens protein-1 (Zo-1). Cell isolation and culture were performed in two laboratories (Department of Biopharmaceutics and Pharmaceutical Technology, Saarland University, Saarbrücken, Germany; Pharmaceutical Cell Biology Welsh School of Pharmacy, Cardiff University, Wales, UK) using the same methods. The average yield of ATII cells was 2.3×10^6 cells/g tissue (n=15). The ATII cell purity determined by staining for alkaline phosphatase was in the range of 81±1%.

A549 cells were obtained from BioWhittaker Europe (Verviers, Belgium). Passage numbers 86–89 were used cultured in Dulbecco's modified Eagle's medium (DMEM) supplemented with 10% FCS in a humidified atmosphere containing 5% CO_2.

Electron microscopy

Fixation

Cells on filter inserts were washed with phosphate-buffered saline (PBS) and fixed with a mixture of 1–4% formaldehyde and 1% glutaraldehyde in 0.1 M phosphate buffer (pH 7.2) at room temperature and stored overnight at 4°C. All formaldehyde solutions were prepared from freshly depolymerized paraformaldehyde. For immunogold electron microscopy cells were washed with PBS and fixed with 4% formaldehyde in acetate buffer (pH 5.6) for 5 min followed by 4% formaldehyde in carbonate buffer (pH 10.8) for 30 min (Berod et al. 1981). After a change to phosphate buffer, the cells were prepared for scanning and transmission electron microscopy using the following protocols. In all preparations cells were left on their original filter substrate.

Scanning electron microscopy of cell surfaces

For scanning electron microscopy cells were dehydrated on their supporting filters through an ethanol gradient (50%, 70%, 80%, 90%, 96%, 99%, 99%, 100%; each for 15 min at room temperature). The drying of samples was prepared by infiltration with mixtures of 1, 1, 1, 3, 3, 3-hexamethyldisilazane (HMDS, Roth, Germany) and ethanol (1:3, 1:1, 3:1, each for 15 min) followed by pure HMDS (twice, each for 15 min). HMDS was removed from the sample by desiccation with a vacuum pump. Dried filters were mounted on aluminium stubs and sputter coated with gold or platinum. Preparations by critical-point drying yielded a similar structural preservation.

Samples were observed using an ESEM XL 30 (FEI, The Netherlands) equipped with a field emission gun at 20–30 kV under high vacuum conditions. For analysis of the filter area covered by cells, digital images were taken randomly at a magnification of ×600. The free filter surface was manually selected and calculated relative to the entire image area using NIH image software (version 1.62, developed at the US National Institutes of Health; customized by Steve Barrett, Surface Science Research Centre, University of Liverpool, UK).

Electron microscopy of cross sections

Cells were washed in 0.1 M phosphate buffer and postfixed with 2% osmium tetroxide in 0.1 M phosphate buffer. After washing in phosphate buffer, cells were dehydrated in a series of ethanol (50%, 70%, 80%, 90%, 96%, 100%, 100%; each for 15 min at room temperature). Infiltration with epoxy resin was done using propylene oxide (twice, each for 5 min; once for 15 min) and a 1:1 mixture of propylene oxide and EMbed 812 (EMS, Fort Washington, USA; resin mixture according to Luft 1961) overnight at room temperature. After a further infiltration step in EMbed for 3–4 h at room temperature, filters were embedded in fresh EMbed and polymerized at 60°C for at least 2 days. Ultrathin sections (60–80 nm thick) were counterstained with uranyl acetate and lead citrate and inspected with an EM10C (Zeiss, Germany).

Low-power images were taken from the block face of embedded filters after sectioning using the scanning electron microscope and imaging of back scattered electrons at 10–15 kV. Blocks were stained with uranyl acetate for a better contrast. This imaging procedure was selected because sections usually show mechanical distortions and artifacts due to the different hardness of embedding medium, cells and filter material.

The general morphology of HAEpC cultured under the described conditions was the same in both laboratories in this study.

Immunogold electron microscopy

Cells were washed with 0.1 M phosphate buffer and dehydrated by progressive lowering of temperature (PLT) using the following ethanol series and temperatures: 30%, 0°C; 50%, –20°C; 70%, 90%, 100%, 100%, –35°C for 1 h each. The incubations were done by using tight-closing vials (2 ml, Twist Top; Sorenson Bioscience), which were placed into different refrigerators and freezers for cooling. At the temperature of –35°C vials were fitted into an aluminium block for a better temperature control.

Infiltration with the acrylate resin Lowicryl K4 M was done at a temperature of –35°C by using mixtures of ethanol and resin (1:1, 1 h; 1:2, 1 h) followed by pure resin (twice; overnight and 2 h). Filter inserts with cells were embedded in fresh resin delivered in reaction vials (0.5 ml, Eppendorf) and polymerized by UV light in a freeze-substitution apparatus (FSU010, Bal-tec) for 1 day at –35°C before the temperature was raised to 0°C (dwell time = 1 day) and room temperature (dwell time = 1 day).

Ultrathin sections were collected on Formvar-filmed copper slot or single hole grids. For immunolabeling, sections were placed on droplets (30 µl) of the following solutions: glycine (50 mM in PBS); blocking solution; anti-caveolin-1 antibody (see below); blocking solution; goat anti-rabbit antibody, coupled to 10 nm colloidal gold (British Biocell, Cardiff, UK); blocking solution; PBS; 2.5% glutaraldehyde in 0.1 M phosphate buffer; PBS; and aqua dest. The blocking solution consisted of cold water fish gelatine (0.5%; Sigma), bovine serum albumin (BSA) (0.5%; Aurion) and Tween 20 (0.01%; Sigma) in PBS. Incubation of sections with the anti-caveolin-1 antibody was done overnight at 4°C in a wet chamber. Finally, dried sections were stained with a mixture of uranyl acetate and methylcellulose (Roth et al. 1990).

For control rabbit non-immune sera were used. Significant labeling of caveolae was never observed with these sera, indicating that the decoration of caveolae by caveolin-1 antibodies was specific.

Antibodies

Caveolin-1 synthesis was examined using the rabbit polyclonal antibody (C-13630, Transduction, Lexington, UK), which recognizes both the α and β isoforms of caveolin-1. Surfactant protein-C (Sp-C) was examined using the rabbit polyclonal anti proSp-C antibody (AB3428, Chemicon, Hofheim, Germany) recognizing the Sp-C proprotein as well as processing intermediates. For the isotypic control an IgG rabbit serum (X0903, Dako, Hamburg, Germany) was used, which was diluted to the protein content of the primary antibodies. Occludin was investigated by mouse monoclonal antibody (O79120, Transduction, Lexington, UK). For detection of intracellular adhesion molecule-1 (ICAM-1), a mouse monoclonal antibody anti human CD54 (CBL 450, Cymbus Biotechnology Ltd., Chandlers Ford, UK) was used. For isotypic controls a mouse IgG antibody (M5284, Sigma, Germany) was diluted to the protein content of the primary antibodies. For Western blotting a secondary horseradish peroxidase (HRP) conjugated swine anti-rabbit antibody (Dako, Cambridge, UK)

was used. For fluorescence labeling cells were incubated with an anti-rabbit $F(ab)_2$FITC conjugate (F1262, Sigma, Deisenhofen, Germany) or an anti-mouse FITC conjugate (F0479, Dako, Hamburg, Germany).

Immunofluorescence confocal microscopy

For immunofluorescence microscopy cells were fixed on Transwell filter inserts with 2% paraformaldehyde and permeabilized by 0.1% Triton-X. Cells were incubated with primary antibodies at room temperature for 40 min in the dark at a dilution of 1:40 in PBS/1% BSA. After the first incubation step the cells were labeled with the corresponding FITC-labeled anti-rabbit or anti-mouse antibody (1:100 in PBS, 1% BSA) for 40 min in the dark. Counterstaining of cell nuclei was undertaken using propidium iodide (0.2 µg/ml). For actin staining fixed and permeabilized cells were incubated with TRITC-phalloidin (P-1951, Sigma, Deisenhofen, Germany) using a concentration of 5 µg/ml in PBS, 1% BSA. Finally cells were mounted in FluorSave (Calbiochem, Darmstadt, Germany) and analyzed using a confocal laser scanning microscope (Biorad MRC 1024, Munich, Germany).

Reverse transcriptase-polymerase chain reaction

The sources for RT-PCR materials were as follows: agarose LE analytical grade and RNasin ribonuclease inhibitor (Promega, Southampton, UK); Ultraspec RNA extraction solution and Ultraspec DEPC-treated water (Biogenesis, Dorset, UK); Moloney murine leukemia virus reverse transcriptase (MMLV-rt) and dNTPs (Life Technologies-Gibco, Paisley, UK); random hexanucleotide (pdN6) primers (AmPharm, Little Chalfont, UK); and Biotaq polymerase (Bioline, UK). Oligonucleotide primers were synthesized within the University of Wales, College of Medicine, on a Beckman DNA synthesizer with high-performance liquid chromatography (HPLC) high-purity isolation.

One microgram RNA was extracted (Ultraspec RNA extraction) from the alveolar epithelial cultures grown on tissue culture-treated plastic Corning Costar and reverse transcribed using 200 units of MMLV-rt and 10 pmol of random pdN6 primers in a solution containing TRIS and $MgCl_2$ (1.5 mM). The cDNA representing 60 ng of RNA was subjected to PCR for human caveolin-1 and glyceraldehyde-3-phosphate dehydrogenase (GAPDH) for 30 cycles in a final volume of 50 µl using 1 unit of Biotaq DNA polymerase and 10 pmol/µl of each primer.

Human caveolin-1 (GenBank accession number Z18951) primers comprised forward 5'-TCA ACC GCG ACC CTA AAC ACC-3'and reverse 5'-TGA AAT AGC TCA GAA GAG ACA T-3' sequences generating a 562-bp product. PCR was undertaken with an $MgCl_2$ concentration of 1.5 mM, a primer concentration of 10 pmol/µl and a thermocycler program of: (1) 95°C for 2 min, (2) 60°C for 1 min, (3) 72°C for 1 min, (4) 95°C for 2 min, (5) 60°C for 1 min, and (6) 72°C for 1 min (steps 4–6 were repeated 26 times) before a final round of 95°C for 1 min, and 60°C for 5 min.

Human GAPDH (GenBank accession number M33197) primers comprised forward 5'-ACC ACA GTC CAT GCC ATC AC-3' and reverse 5'-TCC ACC ACC CTG TTG CTG TA-3' sequences generating a 452-bp product (Hurlstone et al. 1999). PCR was undertaken with an $MgCl_2$ concentration of 1.5 mM, a primer concentration of 10 pmol/µl and a thermocycler program of: (1) 95°C for 2 min, (2) 58°C for 30 s, (3) 72°C for 30 s, (4) 94°C for 1 min, (5) 58°C for 30 s, and (6) 72°C for 30 s (steps 4, 5, and 6 were repeated 28 times) before a final round of 95°C for 1 min, and 58°C for 5 min.

A quantity of 15 µl of the PCR products was electrophoresed in a 2% agarose gel and stained with a solution of ethidium bromide (0.5 µg/ml). Negative controls consisted of omitting the reverse transcription reaction or the cDNA product (data not shown).

Western blot for caveolin-1

Western blot for caveolin-1 in tissues and in cultured cell was performed as previously described (Newman et al. 1999; Campbell et al. 1999).

Flow cytometry

Freshly isolated human alveolar type II cells were directly washed in PBS after the isolation procedure and prepared for flow cytometry. Cells cultured to day 2, 4 and 8 postseeding were trypsinized followed by washing with PBS and prepared for flow cytometry as described below. Cells were fixed and permeabilized using Fix and Perm Kit (GAS-004, Caltag, Hamburg, Germany). Sp-C antibody and caveolin-1 antibody were diluted 1:40 in the permeabilization buffer (buffer B) according to the recommendations. For the isotypic control rabbit IgG normal serum was used. The secondary FITC antibody (F1262) was diluted 1:100 in PBS. After washing, cells were analyzed by flow cytometry using Calibur fluorescence-activated cell sorting (FACS) (BD, Heidelberg, Germany), and CellQuest software. 5000 cells were counted in triplicate for each time point of the primary cultures. Independent isolations from tissue of three patients were subjected to flow cytometry. To exclude any autofluorescence from the cells, instrument settings were adjusted in untreated cells.

To quantify the increase in caveolin-1 and to prove the reproducibility in different isolations, caveolin-1-positive cells were gated as indicated on the dot plot of day 8 cells (Fig. 7A) and the mean FL-1 in the gated population was compared on days 0, 2, 4, and 8 in three isolations. A similar analysis was performed for Sp-C.

Results

Morphology of donor lung tissue

Respiratory parts of human lung tissue were used for preparation of primary cultures. The fine structure of tissue samples revealed the typical architecture of the alveolar epithelium formed by ATII and ATI cells. The ATII cell is cuboidal in shape and its circumference is limited to a zone near the nucleus. The cytoplasm is characterized by multilamellar bodies which are membrane-bound structures containing densely stacked membranes of surfactant lipids (Fig. 1A, B).

ATI cells form flat extensions from a small layer of cytoplasm in the nuclear region. The extensions are a few hundred nanometers in thickness and cover the majority of the inner alveolar epithelial surface. Their apical and basal membranes are invaginated by caveolae (Fig. 1C, D).

Morphology of HAEpC during culture

Isolated ATII cells seeded upon filter membranes, and cultured under the described conditions, formed a confluent monolayer of cells within 10 days of seeding. Cells aggregated, and differentiated during culture into a flattened epithelium consisting of two distinct cell morphologies. The morphology of the cells was analyzed by scanning and transmission electron microscopy (Figs. 2, 3, 4).

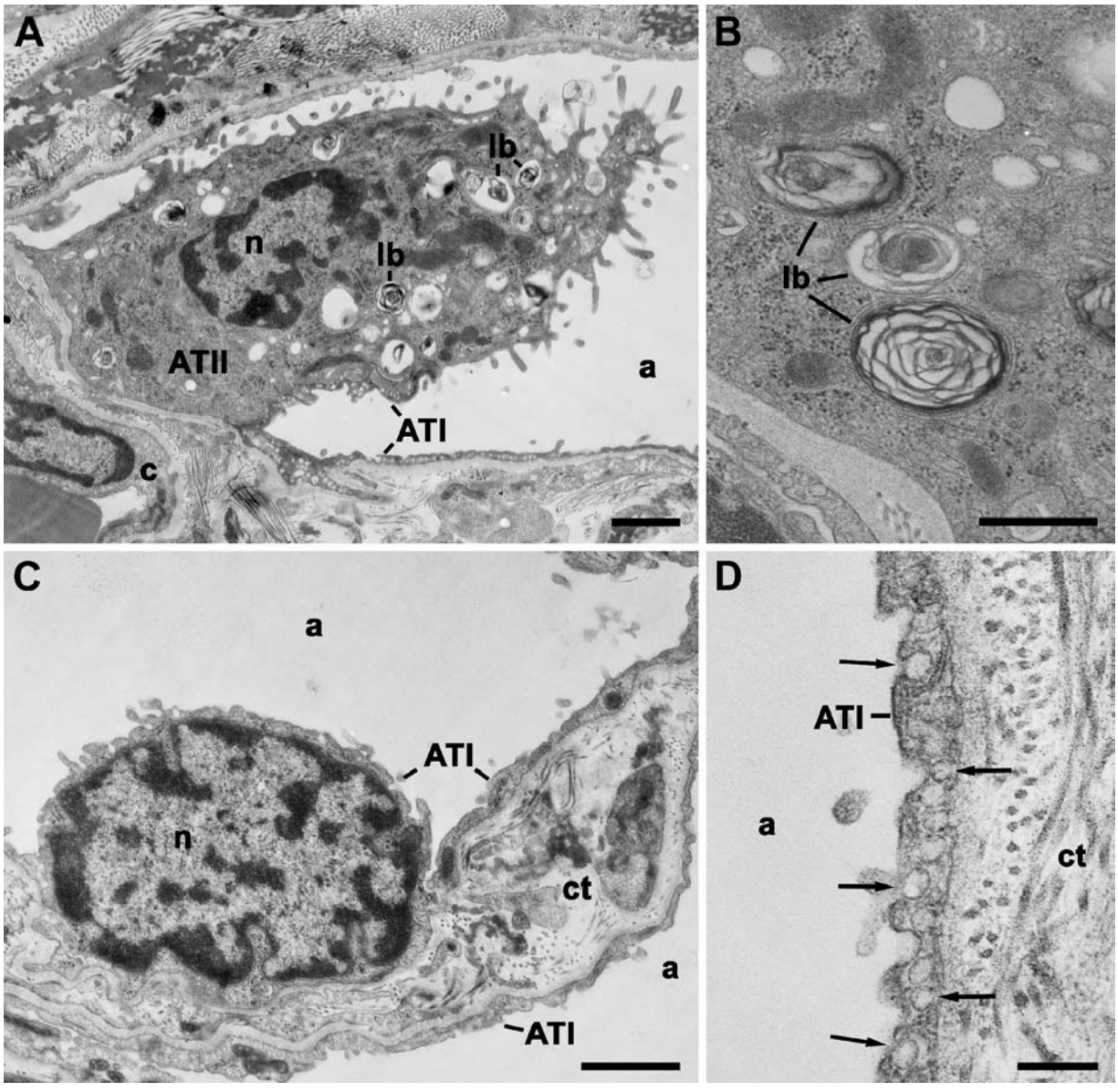

Fig. 1A–D Transmission electron microscopy of donor lung tissue used for primary cell culture of human alveolar epithelial cells. The alveolar epithelium is formed by two cell types, alveolar epithelium type I (*ATI*) and II (*ATII*) cells. **A, B** Section through a cuboidal ATII cell which is elevated above the epithelium. The cytoplasm is characterized by multilamellar bodies (*lb*), membrane-bound structures which reveal densely stacked membrane lamellae. Note that preservation of these structures is not ideal since fixation must be done by immersion several hours after excision of the material. **C, D** ATI cells are flat cells with a thin lamella of cytoplasm around the nucleus. The cells possess flat extensions which cover most of the inner alveolar surface. The apical and basal plasma membranes of these extensions reveal many omega-shaped invaginations, termed caveolae (*arrows*). In some cases caveolae of both membranes approach very closely and are only separated by a few nanometers of cytoplasm from each other (*a* alveolar space, *c* capillary, *ct* connective tissue). *Scale bars* 1 μm **(A, C)**, 0.5 μm **(B)**, 0.2 μm **(D)**

After 2 days of culture, many ATII cells have formed monolayer aggregates which were still separated from each other (Fig. 2A). At this time, more than 40% (n=14) of the filter surface was covered by cells. Cells displayed a morphology consistent with cell flattening and spreading but with a clearly elevated nucleus and a circumference profile that was variable in shape (compare also Fig. 3A, B). The apical surface of the cells was covered by short microvilli, which were most dense in the nuclear region and almost absent in the flattened peripheral region of the cells. Numerous filopodia extended from free lateral cell borders and contacted the surface of the filter or neighboring cells. Closer contacts between cells were characterized by a weakly undulated contact zone formed by the adjacent membranes. The contact zone was on both cells decorated by row(s) of microvilli (compare Fig. 2F).

The intracellular morphology of the cells at day 2 of the culture was relatively uniform. The cytoplasm re-

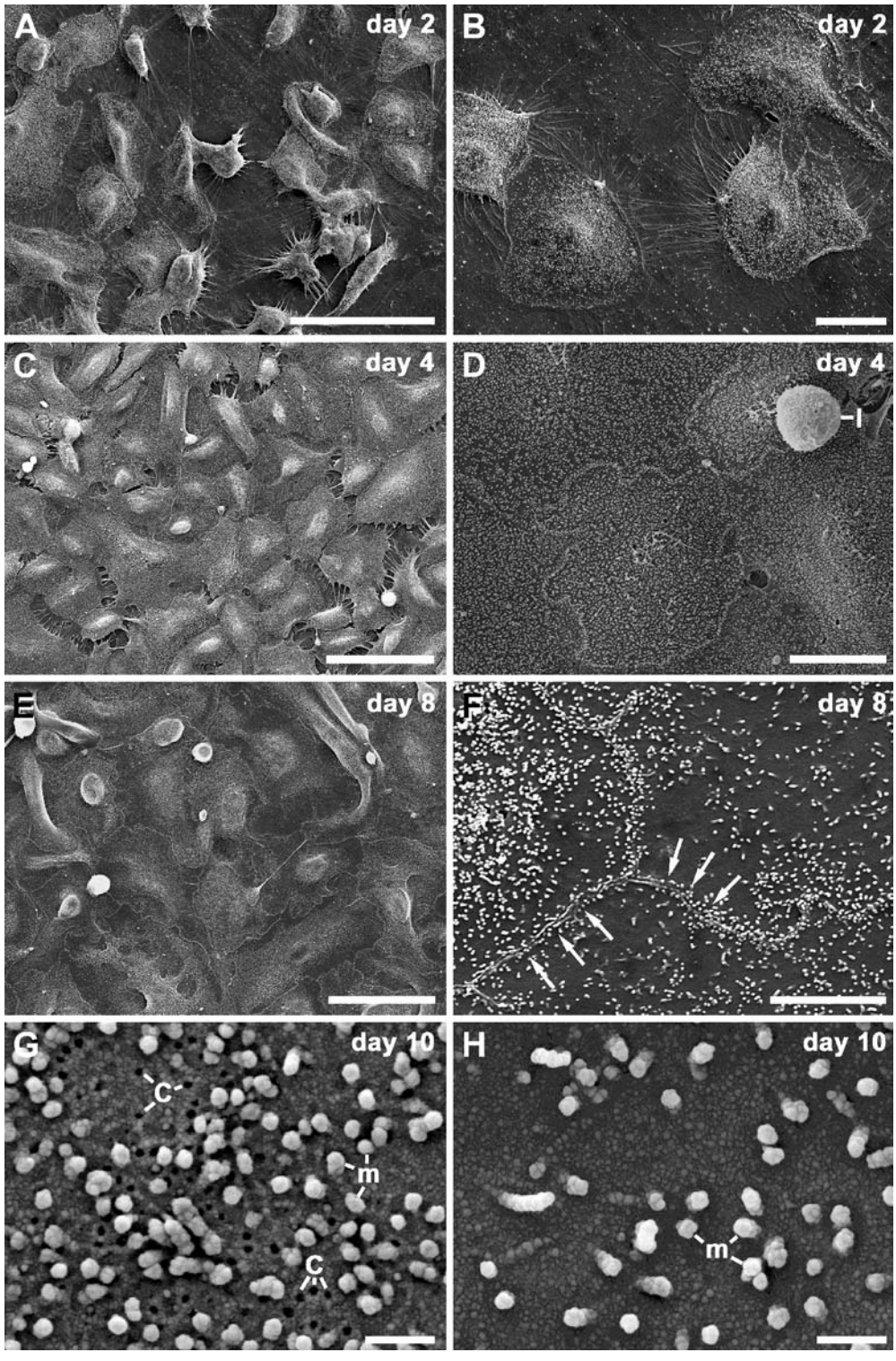

Fig. 2A–H Scanning electron microscopy of cultured human alveolar epithelial cells (HAEpC) after different times of culture. **A, B** On day 2 of culture HAEpC have formed clusters. Cell shape is polymorphic and the cellular surface is characterized by short microvilli. Gaps between cells are spanned by several thin filopodia. **C, D** After 4 days of culture gaps between cells are almost closed. Cells reveal a flat morphology with distinct contact zones between them. **E, F** On day 8, the cells have formed an almost closed monolayer. The cells resemble flat disks of different shapes with slightly elevated nuclei. In many cells surface microvilli are concentrated in the region of the nuclei and are much rarer in the flatter periphery. The contact zone between cells is flanked by one or few rows of microvilli on each cell (*arrows*). **G, H** From day 8 on some cells show surface regions where the membrane is perforated by numerous small concentric holes of a uniform size (*c*). **H** shows the surface of another cell of the same monolayer which is completely devoid of concentric holes. The distribution of membrane holes correlates with that of omega-shaped or flask-like sectioning profiles in ultrathin sections of these monolayers which are indicative of caveolae (cf. text and Fig. 4D). *Scale bars* 50 µm **(A, C)**, 10 µm **(B, D)**, 5 µm **(F)**, 0.5 µm **(G, H)**

vealed no particular concentration of organelles with one exception. Most cells possessed a significant number of membrane-bound organelles of about 0.4–1.2 µm in diameter (maximum sectioning profile; *n*=46). These organelles appeared empty in a few cases, but mostly revealed membranous structures within their lumina (Figs. 3A, B, 4B). In some cells these structures were densely packed membrane lamellae as in ATII cells of the donor tissue (Fig. 4B). Often membrane lamellae seemed to be condensed or reduced and accompanied by vesicular structures (Fig. 4C).

Between islands of cells and single cells of a more or less flattened morphology, a population of smaller round cells of variable diameter and surface structure was ob-

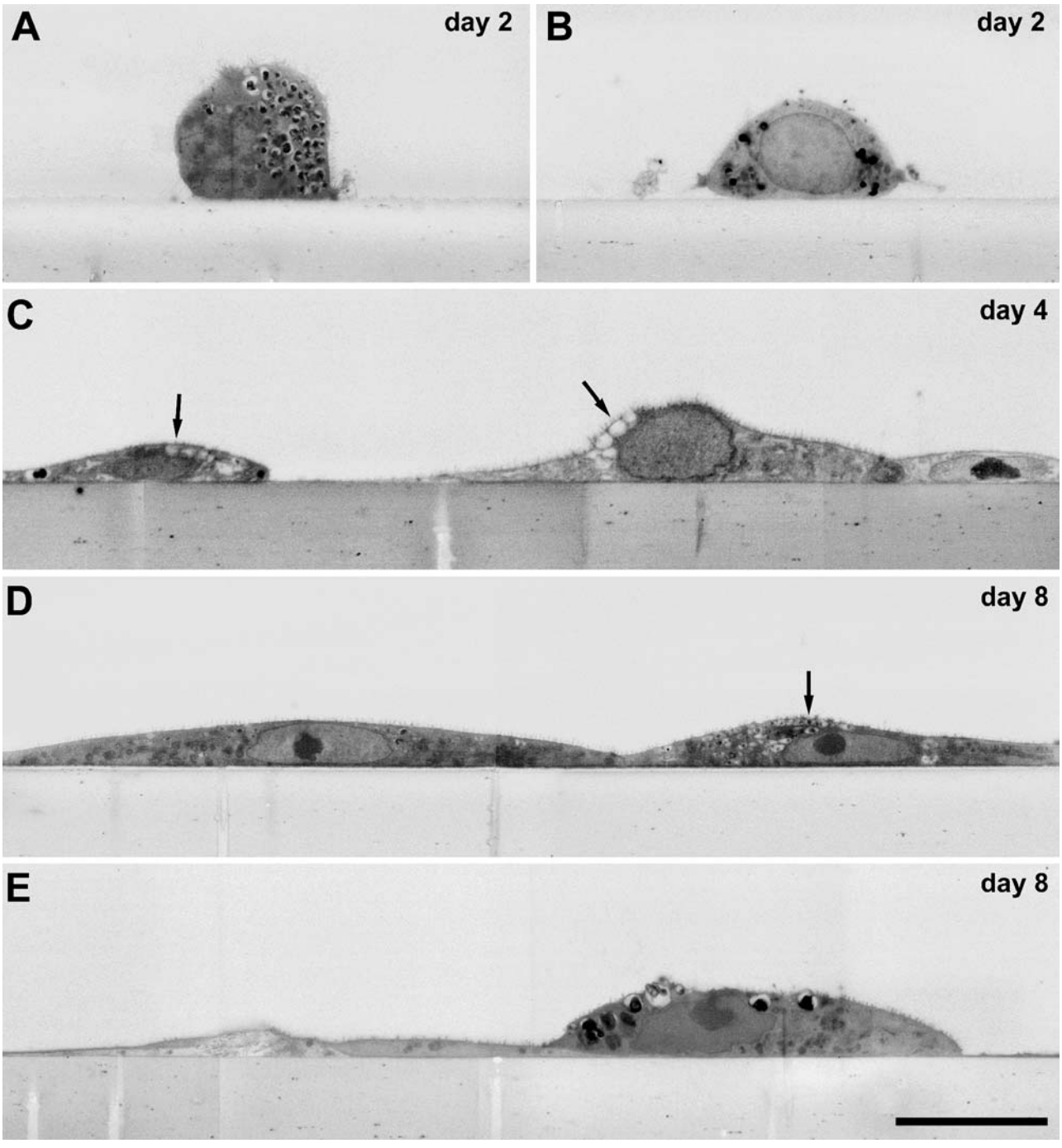

Fig. 3A–E Cross sections through cultured human alveolar epithelial cells (HAEpC) after different times of culture. Plastic-embedded cells were sectioned and the remaining block face was visualized by scanning electron microscopy. **A, B** Single cells with a more or less round sectioning profile and spreading on the filter substrate after 2 days of culture. The cytoplasm reveals electron-dense inclusions which are multilamellar bodies (cf. Fig. 4B). **C** After 4 days of culture cells form a continuous monolayer covering the filter surface. Many cells are characterized by vacuole-like structures (*arrows*) which are filled with vesicles or membrane lamellae (cf. Fig. 4C). **D, E** On day 8 of culture, cells with a flat sectioning profile and flat extensions ("flat cells") cover most of the filter surface. **D** In many of the "flat cells" vacuole-like structures (*arrow*) are present as in cells after 4 days of culture. **E** Occasionally cells with a rounder sectioning profile ("round cells") can be found within the monolayer. These cells contain typical multilamellar bodies. *Scale bar* 10 μm

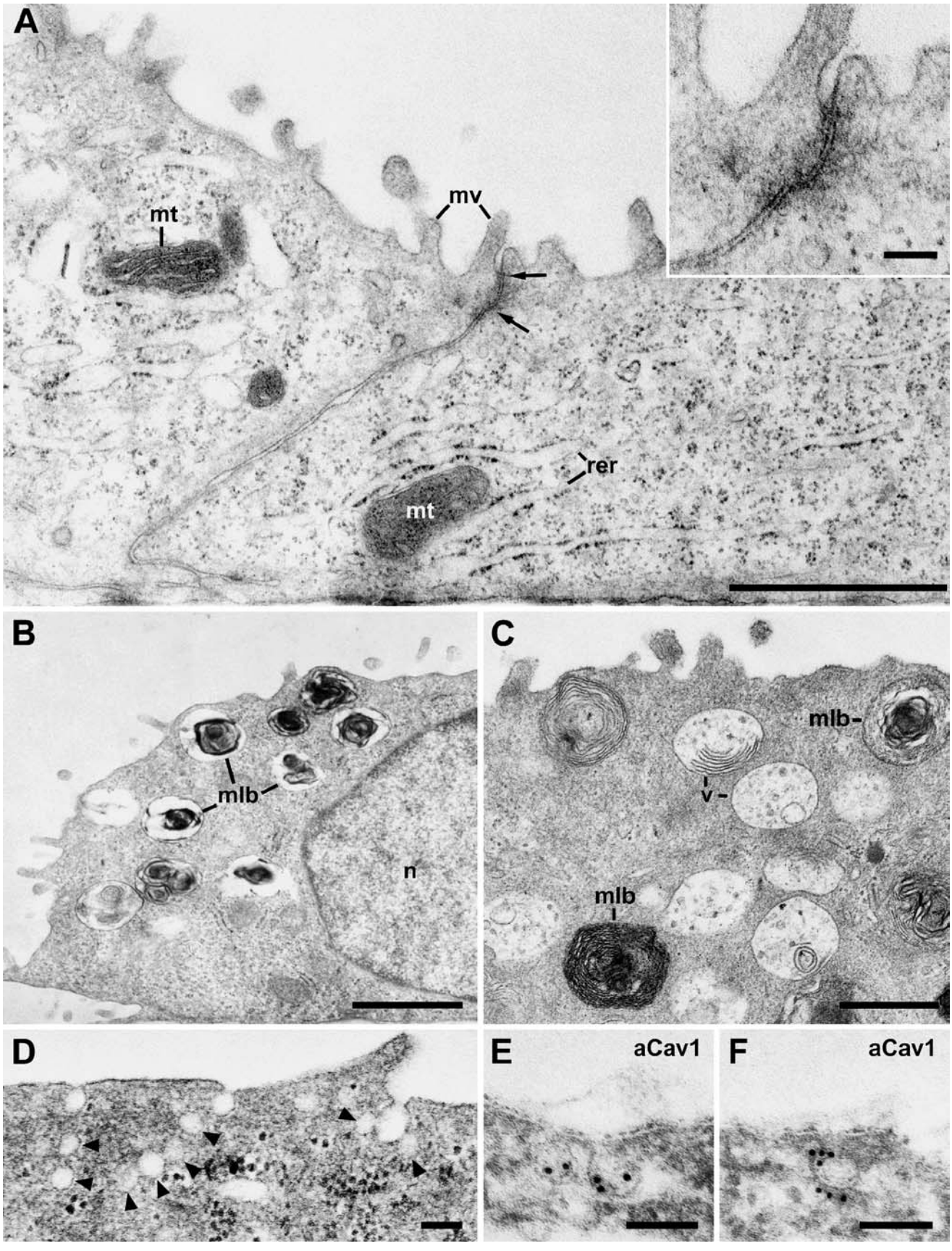
A
mt
mv
rer
mt
B
mlb
n
C
mlb
v
mlb
D
E
aCav1
F
aCav1

served. These cells showed no significant spreading on the substrate, and some of them also laid on the surface of the flattened cells (Fig. 2D). Ultrathin sections revealed a morphology indicative of leukocytes (not shown). Their number seemed to decrease with time of culture. On day 10 of culture none of these cells could be observed.

On day 4 of the culture, gaps between the cells were almost closed. At least 98% (n=15) of the filter surface was covered by cells (Fig. 2C, D). The cell morphology was similar to that of the cells on day 2 with free edges bearing multiple filopodia. Typical apical contact zones, which comprised apical tight junctions sometimes followed by adherent junctions, were much more prominent than on day 2 because cells formed larger contact areas (Fig. 4A). The number of characteristic membrane-bound organelles containing membrane lamellae in their lumina (see above) was lower than in cells on day 2. In most of the cells membrane lamellae seemed to be reduced in size or condensed and were frequently associated with vesicles, which gave the organelles a vacuole-like appearance (Figs. 3C, 4C).

After 8 and 10 days of the culture the cells formed a flat, almost closed monolayer on the filter surface (filter area covered by cells ≥98%, n=16) (Figs. 2B, C, 3D, E). The average thickness of the epithelium was less compared to that of the epithelium on days 2 and 4 (cf. Fig. 3A–E). The remaining gaps between cells were spanned by numerous filopodia of the surrounding cells. The overall density of microvilli was reduced in comparison to cells on day 2 and 4 of culture and seemed to correlate with the thickness of the monolayer. The thinner the monolayer, the lower the density of microvilli. In most cells the flattened peripheral attenuations lacked microvilli. Cell shape remained variable across the monolayer with two distinct classes of cells distinguished based on their cross-section profile and intracellular ultrastructure: (1) cells with a rounder profile ("round cells") and numerous membrane-bound structures containing lamellar membranes (Fig. 3E); and (2) cells with a flattened and extended profile lacking lamellar structures; only membrane-bound structures with condensed membranes were visible in some of these cells. The majority of the filter surface was covered by these "flat cells" (Fig. 3D, E).

In some of the "flat cells" numerous membrane invaginations occurred in restricted regions of the apical plasma membrane. In the scanning electron microscope, they appear as concentric holes of a defined size (mean maximum diameter=45 nm, SD=13, n=135; Fig. 2G, H). Their distribution correlates with the occurrence of omega-shaped or flask-like membrane invaginations in sections which are typical sectioning profiles of caveolae (Fig. 4D). Immunostaining showed that these structures can be specifically labeled by antibodies against caveolin-1, the major structural protein of caveolae (Fig. 4E, F). The total number of caveolae increased from day 8 to 10. Single caveolae were occasionally present in apical membranes of all cells including "round cells."

◀ **Fig. 4A–F** Transmission electron microscopy of cultured human alveolar epithelial cells (HAEpC) in cross section. **A** Two cells of a monolayer after 4 days of culture which show an apical to basolateral polarity and typical epithelial cell contacts, i.e., tight junctions (*arrows*). The *inset* shows a magnification of the cell contacts. **B** Multilamellar bodies (*mlb*) of a cell on day 2 of culture (cf. Fig. 3A, B). The morphology of the multilamellar bodies is comparable to that of multilamellar bodies in ATII cells of the lung (cf. Fig. 2A, B). **C** Multilamellar bodies (*mlb*) and vacuole-like (*v*) structures in a cell on day 4 of culture. The vacuole-like structures contain small vesicles and few membrane lamellae. **D** Flask-like invaginations of the plasma membrane in a "flat cell" which are indicative of caveolae (day 8 of culture). Note that vesicular structures in deeper layers of the cortical cytoplasm (*arrowheads*) seem to be connected to the invaginations of the plasma membrane. **E, F** Immunogold labeling of flask-like membrane invaginations with anti-caveolin-1 (*aCav1*). The gold particles are concentrated around the sectioning profile of the invaginated plasma membrane (*mt* mitochondrion, *mv* microvilli, *rer* rough endoplasmic reticulum). *Scale bars* 1 μm **(A, B)**, 0.5 μm **(C)**, 0.1 μm **(D–F,** *inset*)

Immunofluorescence microscopy

Immunofluorescence studies using a polyclonal anti-caveolin-1 antibody revealed the presence of caveolin-1 in most of the cells after 3 days in culture (Fig. 5A, day 3). Caveolin-1 labeling was seen as fluorescent dots in the cytoplasm. The number of these dots and their size increased with time of the culture (day 9, Fig. 5B). Immunofluorescence studies on A549 cells gave a more diffuse pattern with a fluorescence signal that was weak compared with that in HAEpC at later stages of the culture (Fig. 5E). Moreover, no changes in labeling pattern or intensity of the fluorescence for caveolin-1 were observed during the entire culture.

HAEpC and A549 were also tested for Sp-C in immunofluorescence studies. Sp-C labeling was found in nearly all HAEpC on day 4 (Fig. 5C) with intense staining in the perinuclear region or faint reticular staining throughout the cytoplasm indicating a labeling of the Golgi/ER compartment. In the later stages (day 8), most of cells were nearly negative for Sp-C or revealed single dots in the cytoplasm. Only a few cells on day 8 still showed Sp-C labeling in the area of the Golgi/ER in a pattern similar to that of earlier stages (Fig. 5D). In A549, immunofluorescence for Sp-C resulted in strong staining (Fig. 5F) comparable to the early stages of HAEpC. Intense labeling for Sp-C in these cells was found around the nucleus and in the cytoplasm, where it showed a reticular pattern suggesting a localization of Sp-C in association with the Golgi/ER complex. No change in Sp-C levels or distribution in relation to time of culture of A549 cells was observed, indicating a steady production of Sp-C. Immunofluorescence for the intracellular adhesion molecule ICAM-1 (Fig. 5G) in HAEpC demonstrated an increase in ICAM-1 levels with time of culture. ICAM-1 was situated in small dots, which were either distributed all over the cell or only present the cell periphery.

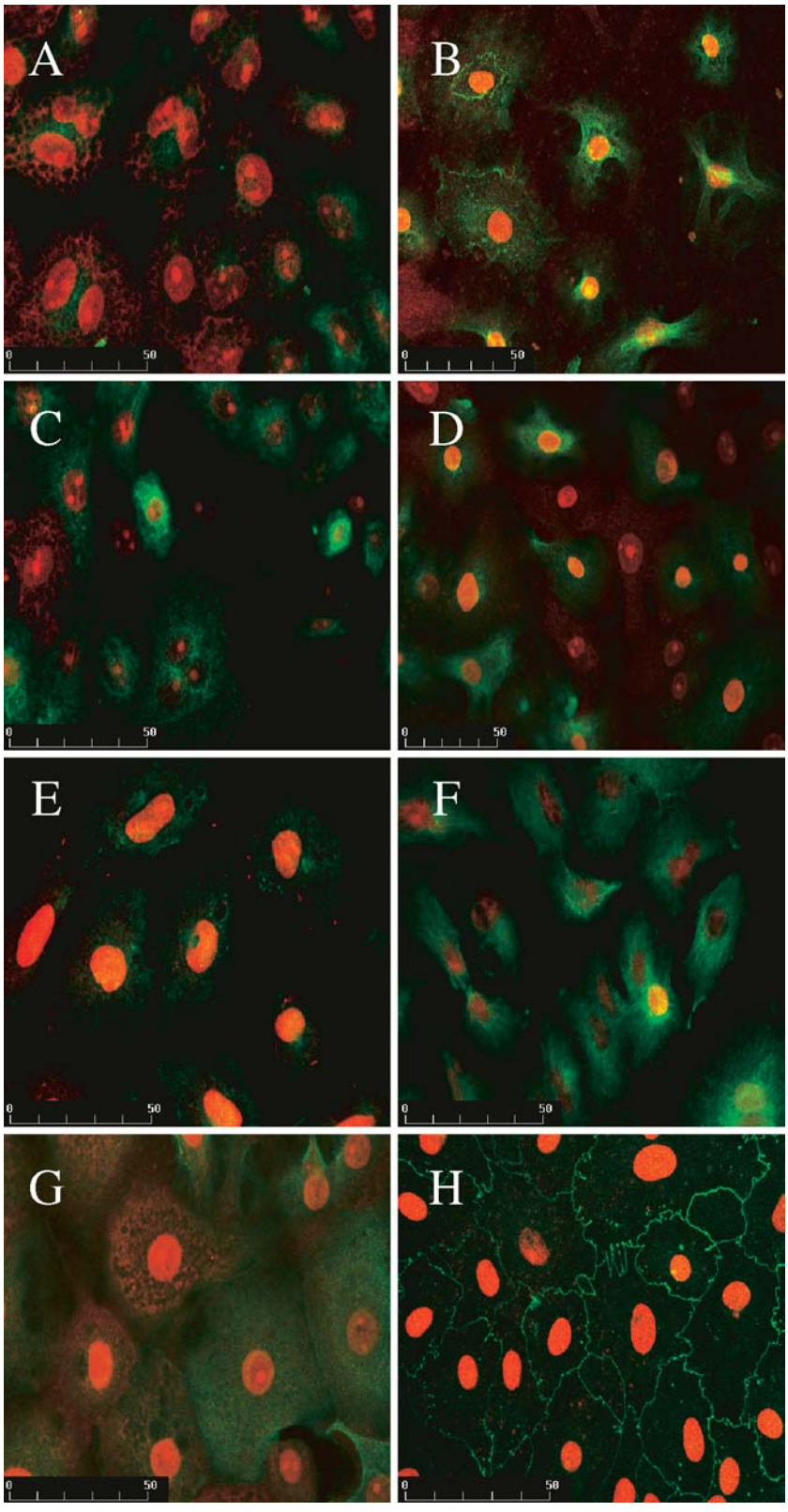

Fig. 5A–H Immunofluorescence of caveolin-1 and Sp-C in HAEpC and A549 cells. Immunoreactivity is displayed in *green* while nuclei appear *red*. **A** HAEpC on day 3 postseeding stained with anti-caveolin-1 antibody reveal weak caveolin-1 levels in HAEpC in nearly all cells. Immunolabeling for caveolin-1 appears in little dots in the cytoplasm. **B** In later stages of the cell culture (day 9) caveolin-1 labeling is situated in dots forming larger aggregates in the cytoplasm and the fluorescence for caveolin-1 is increased. **E** In comparison, A549 cells only display weak fluorescence for caveolin-1 and only a few dots were found in the cytoplasm. No change in caveolin-1 signal during culture time is observed in A549. **C** Immunofluorescence in HAEpC for Sp-C on day 4 postseeding reveals intense staining in nearly all cells. The labeling for Sp-C is particularly intense in the perinuclear region, and extends into the peripheral cytoplasm, where it is reticular with intermingled dots. **D** On day 8 most of the cells are almost negative for Sp-C or reveal only single dots in the cytoplasm. Some cells still reveal an immunofluorescence pattern comparable to the early stages. **F** In A549 cells Sp-C labeling is intense and localized in the perinuclear region, from where it sends reticular strands throughout the cytoplasm similar to the labeling of HAEpC in early stages. Further, A549 show no changes in intensity or concerning the localization of Sp-C during culture time. **G** Immunostaining for ICAM-1 in HAEpC on day 9. ICAM-1 was present in all of the cells but expressed to various extents in single cells. **H** HAEpC stained for occludin on day 9 using a mouse monoclonal antibody. Labeling for occludin demonstrated the formation of continuous circumferential intercellular contacts, which are typical of tight junctions. *Scale bars* **A**–**H** 50 μm

The formation of tight junctions in HAEpC was previously proven by the synthesis of the tight junctional protein zo-1 forming a regular belt around the single cells (Elbert et al. 1999). Immunofluorescence using monoclonal antibodies for occludin (Fig. 5H) and staining of actin filaments by phalloidin-TRITC (not shown) resulted in a very similar labeling. These results indicate the formation of epithelial cell-cell contacts between the cultured cells.

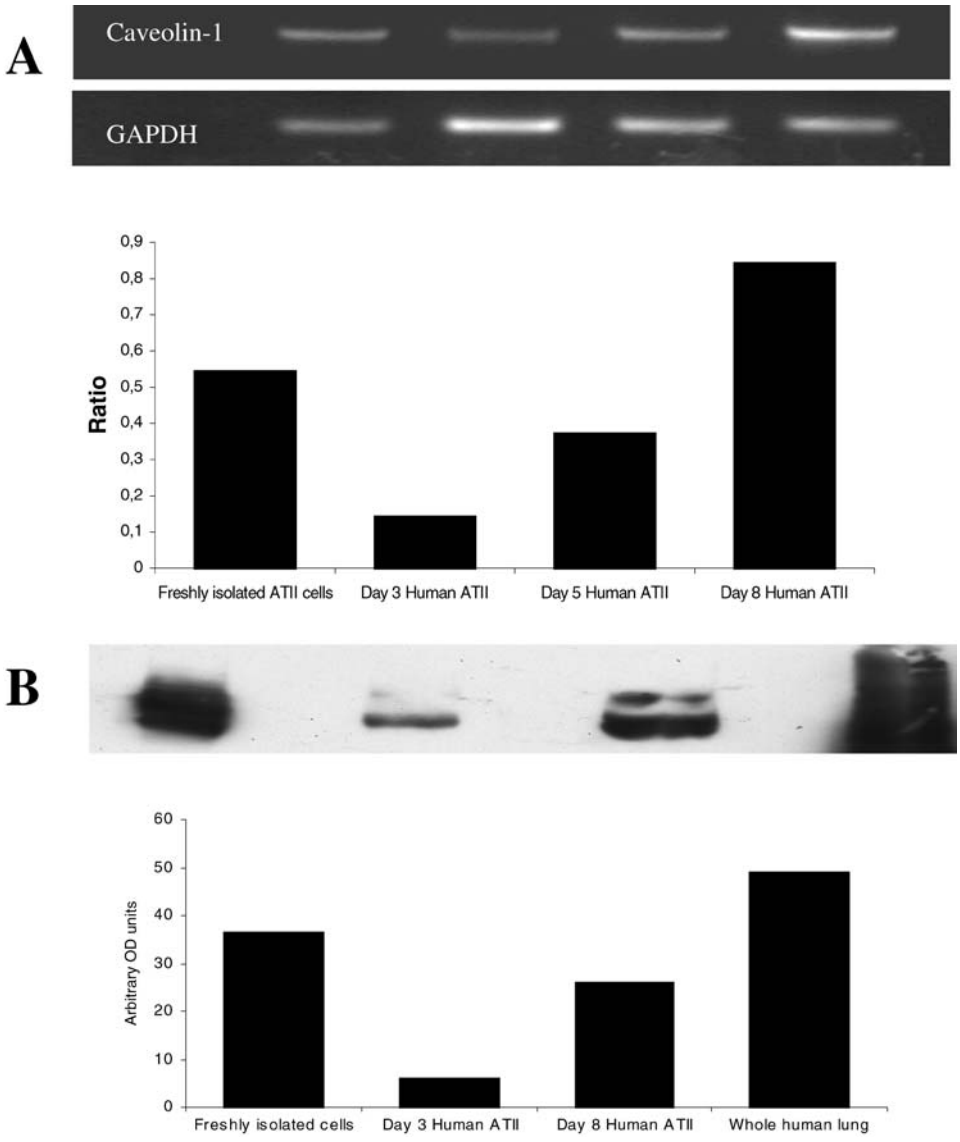

Fig. 6A, B Analysis of caveolin-1 in HAEpC during culture by RT-PCR and immunoblotting. **A** shows RT-PCR for caveolin-1 (from *left to right*) in freshly isolated cells (*lane 1*), and in cells cultured for 3 days (*lane 2*), 5 days (*lane 3*) and 8 days (*lane 4*). GAPDH was used as internal standard. The bands for caveolin-1 are located on the gel at a position consistent with the expected size of 562 bp. Quantification was performed by densitometry analysis upon the above image by determining optical density. The time course reveals relatively high expression rates for caveolin-1 in freshly isolated cells followed by a reduced caveolin-1 expression on day 3. With time of culture a steady increase in caveolin-1 is noticed. **B** Western blotting for caveolin-1 in cells after different times of culture. Human lung lysate was used as control. A double band of 22 kDa is detected. For quantification the optical density per unit area was determined as shown by bar chart. The time course reveals the presence of caveolin-1 in freshly isolated cells. On day 3 the caveolin-1 signal is reduced followed by an increase on day 8

RT-PCR and Western blotting for caveolin-1

The caveolin-1 signal in HAEpC over time of culture was quantified by RT-PCR and Western blotting. Caveolin-1 expression tested at the mRNA level by RT-PCR revealed a product of 562 bp, which was consistent with expected size. GAPDH was used as internal standard. For quantification of the caveolin-1 product, densitometry analysis was performed. The ratio between caveolin-1 and GAPDH was estimated over time of culture. The freshly isolated cells showed a notable expression of caveolin-1 mRNA, which increased from day 3 up to day 8 (Fig. 6A). The same pattern could be found by Western blot analysis (Fig. 6B). Caveolin-1 (22 kDa) was detected in freshly isolated cells and a clear increase in caveolin-1 synthesis from day 3 to day 8 was observed. The positive control, lysate of human lung, revealed a band of the same size.

Flow cytometry

In comparison to other quantitative methods such as RT-PCR and Western blotting, flow cytometry offers the possibility of evaluating the synthesis of marker proteins at the level of a single cell level. This allows discrimination of cell subpopulations according to cell size, granularity and marker proteins. For HAEpC, flow cytometry was done with freshly isolated cells and cells cultured for 2, 4 and 8 days after isolation. In the freshly isolated cells, a weak signal for caveolin-1 was observed (Fig. 7A). The mean of the fluorescence channel FL-1 in the gated population of freshly isolated cells on day 0 was in the range of 50 units. However, in addition to the gated population, other cell populations on the basis of a reduced morphological size (low forward scatter, FSC) and lack of caveolin-1 were detected. On day 2, the caveolin-1 synthesis within the gated HAEpC population

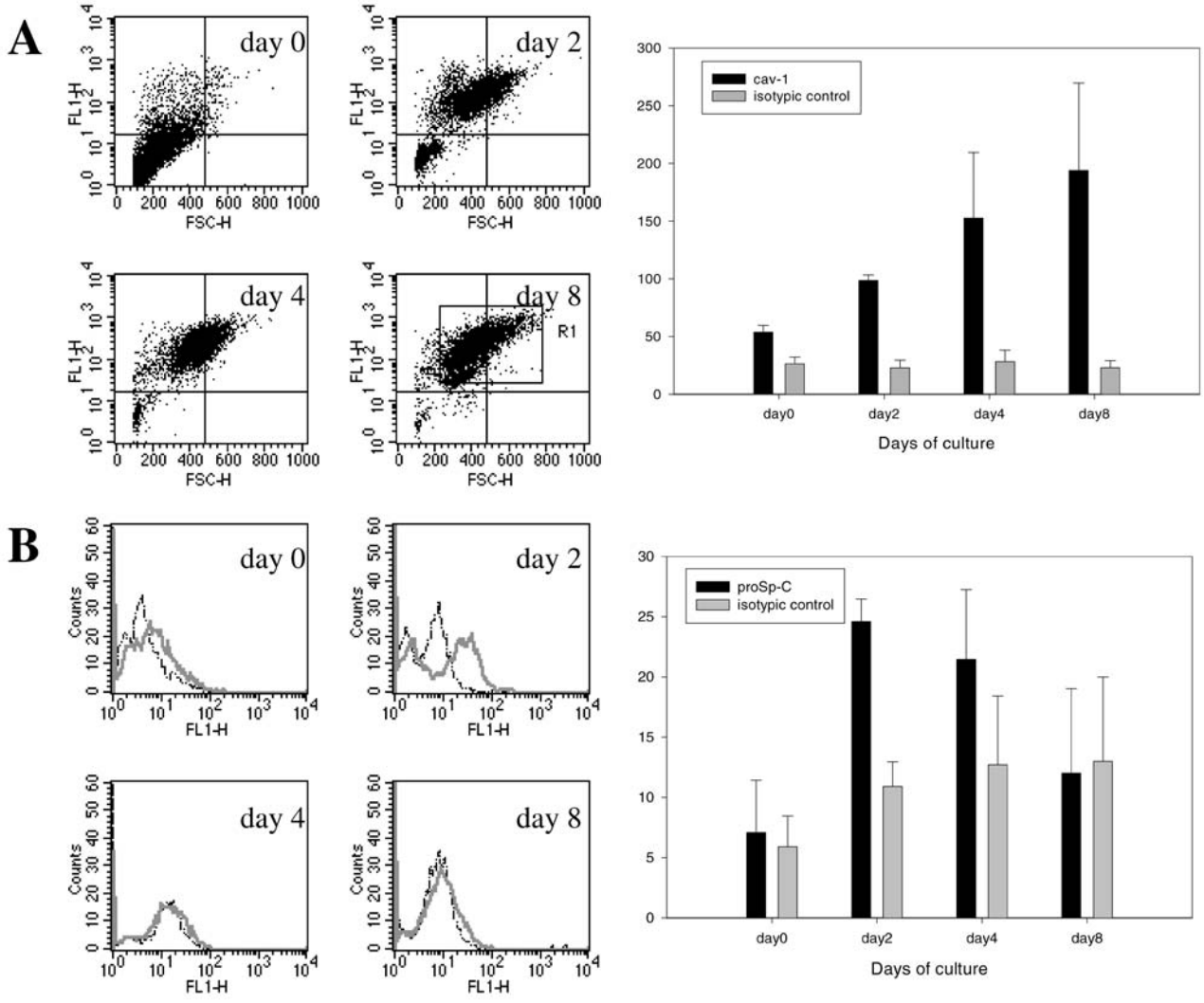

Fig. 7A, B Flow cytometry of caveolin-1 and Sp-C synthesis in HAEpC over time of culture. **A** Time course of caveolin-1 immunoreactivity depicted as dot blot (*left*). Freshly isolated cells reveal a low signal for caveolin-1. Besides HAEpC also other cell populations with lower cell size are detected. With time of culture, caveolin-1 signal increases (days 2, 4). On day 8 HAEpC (gated region is indicated by a *box*) form a homogeneous highly caveolin-1-positive population. In addition the increase in the forward scatter signal suggests an increase in cell size with time of culture. Means for caveolin-1 signal in comparison to the isotypic control determined in three isolates are depicted as a *bar chart on the right*. **B** Time course for Sp-C (*gray line*) depicted in histograms (*left*) compared to the isotypic control (*black line*). In freshly isolated cells no Sp-C is detected. On day 2 the signal for Sp-C increases and reaches a maximum. On day 4 HAEC show a decrease in Sp-C expression. On day 8 no signal for Sp-C is detected. The mean of Fl-1 for Sp-C was determined in comparison to isotypic control in three isolates and depicted as a *bar chart on the right*

was increased significantly and the cells formed a homogeneous caveolin-1-positive population. On day 4 and day 8 caveolin-1 levels within the gated cells had increased further. In addition, the entire population was more homogeneous with over 90% of the cultured cells represented within the gated population and showed high levels of caveolin-1. Other subpopulations of lower size and insignificant caveolin-1 signals disappeared, indicating that they may constitute erythrocytes, leukocytes or other irrelevant cells. On day 10 no further increase in caveolin-1-specific fluorescence was detectable (not shown). In addition to the increase in caveolin-1 synthesis, an increase in cell size was also detected consistent with flattening and cell spreading. Means of FL-1 were determined from three cell isolates (Fig. 7A).

As a control, FACS analysis was performed with A549 cells. These cells formed homogeneous cell populations and showed high levels of Sp-C and low levels of caveolin-1, which corresponds to an ATII cell pattern. The intensity of the FL-1 signal for caveolin-1 or respectively Sp-C was not influenced by culture time in this cell line (data not shown).

Sp-C, an ATII cell marker, was screened in HAEpC by flow cytometry over time of culture. A representative time course for Sp-C FACS analysis is depicted in Fig. 7B. In freshly isolated cells only a faint FL-1 signal for Sp-C was present. On day 2, the signal for Sp-C increased and reached a maximum for the analyzed time course of the culture. On day 4 Sp-C levels decreased

slightly and disappeared on day 8. The means of Sp-C were determined in three isolates (Fig. 7B).

Discussion

The morphological investigation of HAEpC at different time points postseeding showed that cells form an epithelial monolayer with typical cell contacts and an apical to basal polarity. The formation of an epithelial barrier is indicated by high TEER values and immunolocalization of cell contact proteins zo-1, and occludin together with cortical actin (compare also Elbert et al. 1999), which are critical components in the formation of tight junctions (Fanning et al. 1998). In addition to the development of an overall epithelial morphology, cells differentiate into two types. On day 2 postseeding the culture is mainly characterized by cells of variable shape but with a clearly elevated nucleus. These cells possess numerous organelles containing membrane lamellae which reveal a close similarity to the typical multilamellar bodies storing surfactant components in cuboidal ATII cells present in the donor tissue. On days 8 and 10 of culture two cell types could be distinguished within the epithelial monolayer: (1) "round cells" retaining a rounder cell shape and (2) "flat cells" covering the majority of the filter surface. Both cell types revealed a morphological similarity with the two alveolar cell types forming the epithelium in the lung and therefore can be termed ATII- and ATI-like cells respectively. In particular, the ATII-like cell revealed a similar morphology to the predominant cell type on day 2 of culture, which most likely represents the isolated ATII cells (see above). ATI-like cells are flat and cover most of the filter surface, similar to ATI cells in the alveolar epithelium. In addition, ATI-like cells developed plasma membrane invaginations which possessed typical features of caveolae, i.e., an omega-shaped or flask-like sectioning profile and a cross-reaction with antibodies against caveolin-1. Both aspects, the flat morphology and the occurrence of caveolae, are features of ATI cells of the alveolar epithelium. However, ATI-like cells are still considerably thicker than ATI cells and the number of caveolae is also comparatively low in ATI-like cells. Moreover, in ATI-like cells vacuole-like structures were often observed which are reminiscent of residual or incomplete multilamellar bodies of the ATII cells. The morphology of the ATI-like cells could represent a snapshot of the hypothesized differentiation process from the ATII-cell type towards the ATI cell type (Uhal 1997; Fehrenbach 2001), where the ATI-like cells show characteristics of both ATII and ATI cell types, i.e., a flat morphology with increasing number of caveolae (ATI cell) and residual multilamellar bodies (ATII cell). This notion is supported by the morphological observations of cells on day 4 of culture, which show a flatter morphology than cells on day 2 and an overall reduced number of intact multilamellar bodies. On day 4 of culture the filter area is already entirely covered by cells which might mark the end of the growth phase and the beginning of the differentiation process into different cell types.

The morphological differentiation of the HAEpC is accompanied by a change in the synthesis of marker proteins for the two cell types of the alveolar epithelium. Caveolin-1 has been proposed as a marker that is selectively increased in the ATI cell (Campbell et al. 1999; Newman et al. 1999). The results from RT-PCR suggest an increase in caveolin-1-specific mRNA during the culture. This was also seen at the protein level for caveolin-1 in Western blotting. In parallel, an increase in caveolin-1 was also observed by immunofluorescence studies and flow cytometry over the time course of the culture. Significant differences in caveolin-1 levels were only found within freshly isolated cells investigated by different methods. In freshly isolated cells a relatively high signal for caveolin-1 was observed by RT-PCR and Western blotting, whereas in flow cytometry the signal for caveolin-1 was weak. This discrepancy might be due to contaminating subpopulations of cells, such as endothelial cells (rarely seen by electron microscopy) or fibroblasts, within the freshly isolated ATII cells, which were selectively excluded by FACS settings but included within RT-PCR and Western blot analysis. However, all results show an increase in caveolin-1 over time of cultivation, which is, according to the flow cytometry data, concentrated in a growing population of cells. This result is in good correlation with the morphology of the cultivated cells which achieve ATI-like properties over time like caveolae and an increase in surface area covered by an individual cell. An increase in the forward scatter (FSC) signal in FACS analysis indeed showed that highly caveolin-1-positive cells also increase in cell size on days 4 and 8 of the culture.

Caveolae may play a fundamental role in macromolecule absorption from the lung alveolar air space and in regulation or maintenance in the alveolar type I phenotype. Recent data from caveolin-1 knockout mice (Drab et al. 2001; Razani et al. 2001) and more recently from caveolin-2 knockout mice (Razani et al. 2002) support the role of caveolin-1 serving as a key structural protein for caveolae formation. The knockout mice studies revealed that loss of caveolin-1 led to exercise intolerance and severe morphological changes in the alveolar barrier including hyperproliferation, thickening of the alveolar septa and ATII hyperplasia. The recent publication by Razani et al. (2002) shows that loss of caveolin-2 appears to be responsible for the pulmonary defects detected in the knockout mice.

The synthesis of the ATII cell marker Sp-C was restricted to the earlier stages of HAEpC cultures (days 2 and 4) as shown by flow cytometry. In the later cultures (day 8) the Sp-C signal was reduced, which can be correlated with the morphological observation of a reduced number of cells with intact multilamellar bodies. Although we expected high rates of Sp-C as ATII marker in freshly isolated cells, Sp-C signal in freshly isolated cells was low, which might be due to the loss of the soluble Sp-C during isolation and the mechanical stress by the

long isolation process. Indeed, Wirtz and Dobbs (1990) previously reported surfactant release after mechanical stretching of ATII cells, which can be explained by the in vivo function of surfactant to lower the surface tension. Low levels of Sp-C in freshly isolated cells might also result from a downregulation of surfactant production during the isolation and its new initiation in the early stages of the culture. Confocal microscopy revealed a change in the localization of Sp-C from the Golgi/ER around the nucleus to distal subcellular compartments where the proprotein is processed into the mature Sp-C peptide of 3.7 kDa as previously reported by Beers and Lomax (1995) and Vorbroker et al. (1995). In addition to the change in the localization of Sp-C, similar time patterns for Sp-C expression were described by Borok et al. (1998) at the mRNA level with Sp-C expression also restricted to days 4 and 6 in primary cultures of rat cells. Nevertheless, downregulation of the Sp-C production on days 4 and 8 can be explained by the beginning of differentiation of ATII cells into ATI-like cells, which is indicated by the morphology and caveolin-1 expression as described above. The differentiation from ATII to ATI-like cells is also supported by the increase in ICAM-1 with time of culture as revealed by immunofluorescence microscopy. The transmembrane adhesion molecule ICAM-1 is constitutively expressed on the apical surface of ATI cells in vivo and in culture the shift from a dominant ATII phenotype to a dominant ATI phenotype correlates with an increase in ICAM-1 expression (Christensen et al. 1993; Rosseau et al. 2000).

In summary, our study demonstrated a differentiation process of the HAEpC with ongoing culture. The late cultures (days 8 and 10) of HAEpC develop morphological and molecular features which are of basic importance for the alveolar epithelium in vivo. A good correlation between the morphological findings in the donor tissue, resembling the in vivo situation, and the differentiated HAEpC was shown. These results suggest that HAEpC might be suitable as an in vitro model to investigate cell biological processes and transport mechanisms with pharmaceutical implications in human alveolar cells. A key element relevant for pharmaceutical studies are caveolae, which are supposed to be involved in molecular transport across the epithelium. In this context, the human alveolar epithelial cell culture model described here may allow elucidation of caveolae-mediated transport in the lung, which might be used as a new approach in drug delivery via the pulmonary route.

Acknowledgements The Department of Thoracic and Cardiovascular Surgery, Saarland University, Homburg, Germany (Prof. Dr. H.-J. Schäfers) and the Clinic for Thoracic and Cardiovascular Surgery in Völklingen, Germany (Dr. H. Isringhaus, Dr. H. Huwer), are thanked for the supply of human biopsies. We finally thank Norbert Pütz, Birgit Leis, Gabi Kiefer, Heike Stumpf and Roland Fuchs for their excellent technical assistance.

References

Alcorn JL, Smith ME, Smith JF, Margraf LR, Mendelson CR (1997) Primary culture of human type II pneumocytes: maintenance of a differentiated phenotype and transfection with recombinant adenovirus. Am J Respir Cell Mol Biol 17:672–682

Beers MF, Lomax C (1995) Synthesis and processing of hydrophobic surfactant protein C by isolated rat type II cells. Am J Physiol 269:L744–753

Beers MF, Kime CY, Dodia C, Fisher AB (1994) Localization, synthesis, and processing of surfactant protein SP-C in rat lung analyzed by epitope-specific antipeptide antibodies. J Biol Chem 269:20318–20328

Berod A, Hartman BK, Pujol JF (1981) Importance of fixation in immunohistochemistry: use of formaldehyde solutions at variable pH for the localization of tyrosine hydroxylase. J Histochem Cytochem 29:844–850

Borok Z, Lubman RL, Spencer ID, Zhang XL, Zabski SM, King LS, Lee DM, Agre P, Crandall ED (1998) Keratinocyte growth factor modulates alveolar epithelial cell phenotype in vitro: expression of aquaporin 5. Am J Respir Cell Mol Biol 18:554–561

Campbell L, Hollins AJ, Al Eid A, Newman GR, Ruhland von C, Gumbleton M (1999) Caveolin expression and caveolae biogenesis during transdifferentiation in lung alveolar epithelial primary cultures. Biochem Biophys Res Com 262:744–751

Cheek JM, Evans MJ, Crandall ED (1989) Type I cell-like morphology in tight alveolar epithelial monolayers. Exp Cell Res 184:375–387

Christensen PJ, Kim S, Simon S, Toews G, Paine R III (1993) Differentiation related expression of ICAM-1 by rat alveolar epithelial cells. Am J Respir Cell Mol Biol 8:9–15

Crapo JD, Barry BE, Gehr P, Bachhofen M, Weibel ER (1982) Cell number and cell characteristics of normal human lung. Am Rev Respir Dis 125:332–337

Cunningham AC, Zhang JG, Moy JV, Ali S, Kirby JA (1997) A comparison of the antigen-presenting capabilities of class II MHC-expressing human lung epithelial and endothelial cells. Immunology 91:458–463

Danto SI, Zabski SM, Crandall ED (1992) Reactivity of alveolar cells in primary culture with type I monoclonal antibodies. Am J Cell Mol Biol 6:296–306

Danto SI, Shannon JM, Borok Z, Zabski SM, Crandall ED (1995) Reversible transdifferentiation of alveolar epithelial cells. Am J Respir Cell Mol Biol 12:497–502

Dobbs LG, Williams MC, Gonzales R (1988) Monoclonal antibodies specific to apical surfaces of rat alveolar type I cells bind to surfaces of cultured, but not freshly isolated, type II cells. Biochim Biophys Acta 970:146–156

Dobbs LG, Pian MS, Maglio M, Dumars S, Allen L (1997) Maintenance of the differentiated type II cell phenotype by culture with an apical air surface. Am J Physiol 273:L347–354

Drab M, Verkade P, Elger M, Kasper M, Lohn M, Lauterbach B, Menne J, Lindschau C, Mende F, Luft FC, Schedl A, Haller H, Kurzchalia TV (2001) Loss of caveolae, vesicular dysfunction and pulmonary defects in caveolin-1 gene-disrupted mice. Science 293:2449–2452

Elbert KJ, Schäfer UF, Schäfers HJ, Kim KJ, Lee VH, Lehr CM (1999) Monolayers of human alveolar epithelial cells in primary culture for pulmonary drug absorption and transport studies. Pharm Res 16:601–608

Fanning AS, Jameson BJ, Jesaitis LA, Anderson JM (1998) The tight protein zo-1 establishes a link between the transmembrane protein occluding and the actin cytoskeleton. J Biol Chem 273:29745–29753

Fehrenbach H (2001) Alveolar epithelial type II cell: defender of the alveolus revisited. Respir Res 2:33–46

Giard DJ, Aaronson SA, Tordaro GJ, Arnstein P, Kersey JH, Dosik H, Parks WP (1973) In vitro cultivation of human tumors: establishment of cell lines derived from a series of solid tumors. J Natl Cancer Inst 51:1417–1423

Godfrey RAW (1997) Human airway epithelial tight junctions. Microsc Res Techn 38:488–499

Gumbleton M, Abulrob AG, Campbell L (2000) Caveolae: an alternative transport compartment. Pharm Res 17:1035–1048

Hurlstone AF, Reid G, Reeves JR, Fraser J, Srtathdee G, Rahilly M, Parkinson EK, Black DM (1999) Analysis of the caveolin-1 gene at human chromosome 7q31.1 in primary tumours and tumour derived cell lines. Oncogene 18:1881–1890

Kalina M, Mason RJ, Shannon JM (1992) Surfactant protein C is expressed in alveolar type II cells but not in Clara cells of rat lung. Am Respir J Cell Mol Biol 6:594–600

Kasper M, Reimann T, Hempel U, Wenzel KW, Bierhaus A, Schuh D, Dimmer V, Haroske G, Mueller M (1998) Loss of caveolin-1 expression in type-I pneumocytes as an indicator of subcellular alterations during fibrogenesis. Histochem Cell Biol 109:41–48

Kreda SM, Gynn M, Fenstermacher DD, Boucher RC, Gabriel SE (2001) Expression and localization of epithelial aquaporins in the adult human lung. Am J Respir Cell Mol Biol 24: 224–234

Luft JH (1961) Improvements in epoxy resin embedding methods. J Biophys Biochem Cytol 9:409–416

Mathias NR, Yamashita F, Lee VHL (1996) Respiratory epithelial cell culture models for evaluation of ion and drug transport. Adv Drug Deliv Rev 22:215–249

Newman GR, Campbell L, Ruhland von C, Jasani N, Gumbleton M (1999) Caveolin and its subcellular immunolocalization in lung epithelium: implications for alveolar type I cell function. Cell Tissue Res 295:111–120

Phelps DS, Floros J (1991) Localization of pulmonary surfactant proteins using immunohistochemistry and tissue in situ hybridization. Exp Lung Res 17:985–995

Razani B, Engelman JA, Wang XB (2001) Caveolin null mice are viable but show evidence of hyperproliferative and vascular abnormalities. J Biol Chem 276:38121–38138

Razani B, Wang XB, Engelman JA, Battista M, Lagaud G, Zhang XL, Kneitz B, Hou H Jr, Christ GJ, Edelmann W, Lisanti MP (2002) Caveolin-2-deficient mice show evidence of severe pulmonary dysfunction without disruption of caveolae. Mol Cell Biol 22:2329–2344

Rosseau S, Selhorst J, Wiechmann K, Leissner K, Maus U, Mayer K, Grimminger F, Seeger W, Lohmeyer J (2000) Monocyte migration through the alveolar epithelial barrier: adhesion molecule mechanisms and impact of cytokines. J Immunol 164:427–435

Roth J, Taatjes DJ, Tokuyasu KT (1990) Contrasting of Lowicryl K4 M thin sections. Histochemistry 95:123ff

Uhal BD (1997) Cell cycle kinetics in the alveolar epithelium. Am J Physiol 272:L1031–1045

Wirtz HR, Dobbs LG (1990) Calcium mobilization and exocytosis after one mechanical stretch of lung epithelial cells. Science 250:1266–1269

Vanderbilt JN, Dobbs LG (1998) Characterization of the gene and the promoter for RTI40, a differentiation marker of type I alveolar epithelial cells. Am J Respir Cell Mol Biol 19:662–671

Vorbroker DK, Voorhout WF, Weaver TE, Whitsett JA (1995) Posttranslational processing of surfactant protein C in rat type II cells. Am J Physiol 259:L727–L733